THE AMERICAN SOCIETY OF MECHANICAL ENGINEERS
345 E. 47th St., New York, N.Y. 10017

98-GT-576

ACTIVE CONTROL OF COMBUSTION FOR OPTIMAL PERFORMANCE

Mathew D. Jackson and Ajay K. Agrawal[1]
Gas Turbine Systems Laboratory
School of Aerospace and Mechanical Engineering
University of Oklahoma, Norman, OK 73019

ABSTRACT

Combustion-zone stoichiometry and fuel-air premixing were actively controlled to optimize the combustor performance over a range of operating conditions. The objective was to maximize the combustion temperature, while maintaining NOx within a specified limit. The combustion system consisted of a premixer located coaxially near the inlet of a water-cooled shroud. The equivalence ratio was controlled by a variable-speed suction fan located downstream. The split between the premixing air and diffusion air was governed by the distance between the premixer and shroud. The combustor performance was characterized by a cost function evaluated from time-averaged measurements of NOx and oxygen concentrations in products. The cost function was minimized by the downhill simplex algorithm employing closed-loop feedback. Experiments were conducted at different fuel flow rates to demonstrate that the controller optimized the performance without prior knowledge of the combustor behavior.

INTRODUCTION

With increasing concerns for air quality improvement, the combustion systems are undergoing major design changes to reduce the harmful by-products. In particular, emphasis has been placed on reducing emissions of nitrogen oxides (NOx) coincident with high combustion efficiency to decrease carbon monoxide (CO), unburnt hydrocarbons (UHC) and soot etc. Techniques to reduce NOx formed by the thermal mechanism usually involve lowering the combustion temperature, for example, by lean-premixed combustion. Although low-emission combustion systems are designed to operate efficiently at specified conditions, a particular challenge lies in achieving optimal performance at off-design operations. The operating conditions differ from the design point because of the part-load operation or changes in the inlet conditions due to ambient, fuel composition etc. Furthermore, a combustor design will not be optimal as new emission standards are introduced. Active control provides the means to adapt the combustor design to changes in the operating conditions.

The most common application of active techniques in combustion has been the control of pressure oscillations by continuously perturbing certain parameters in response to filtered outputs from sensors placed in the combustor (McManus et al., 1993; Wilson et al., 1995; Kemal and Bowman, 1996; Neumeier and Zinn, 1996). An application to improve the gas turbine combustor performance by actively controlling the fuel atomizing airflow rate was demonstrated by Brouwer et al. (1990). Although a single input was controlled, the combustor performance in practice is affected by several parameters requiring trade-off to achieve an optimal design.

Padmanabhan et al. (1995) implemented an active optimal control strategy to simultaneously control the volumetric heat release and pressure fluctuations in a laboratory-scale combustor. Measurements of pressure oscillation and heat release were used to quantify the performance in terms of a cost function, which was minimized by seeking the optimal combination of input parameters; periodic forcing of the boundary layer at the inlet, and crossflow jets upstream of the inlet. Recently, Davis and Samuelsen (1996) evaluated a similar approach to optimize performance of a model gas turbine combustor over a range of load conditions (or duty cycle) by articulating the geometry. The split between the dome airflow and primary jet airflow was controlled using variable area flow restrictors. The cost was evaluated from a weighted sum of the measured combustion efficiency and NOx emissions.

In this paper, we introduce active control to optimize the combustor performance at different operating conditions by articulating the fuel-air premixing and combustion-zone stoichiometry. Recent combustor designs have involved manipulation of these parameters to achieve low-emissions (Maughan et al., 1997, Puri et al., 1997, Yamada et al., 1997). Our combustion system is a burner used in residential furnaces. However, it represents some of the essential features of lean-premixed combustors used in advanced gas turbines. We employ the concept of

[1] Associate Member of ASME, Corresponding Author

Presented at the International Gas Turbine & Aeroengine Congress & Exhibition
Stockholm, Sweden — June 2–June 5, 1998
This paper has been accepted for publication in the Transactions of the ASME
Discussion of it will be accepted at ASME Headquarters until September 30, 1998

control presented by Padmanabhan et al. (1995) although the implementation on the combustor, sensors, and actuators are different. In the following sections, we provide the experimental details, show results to demonstrate the controller, and summarize our findings.

EXPERIMENTAL SETUP

The experimental setup consisted of the combustion system, instrumentation, and control system as discussed below.

Combustion System

The combustor chosen for this study is a burner used in residential furnaces (Kolluri et al., 1996). A schematic of the combustion system is shown in Fig. 1. The ambient air is entrained by the fuel ejected from a nozzle and subsequently, a fuel-air mixture is formed in the converging-diverging tube (or the premixer). The entrained air is denoted as the premixing air or primary air. The fuel-air mixture emerges from 12 equally spaced holes at the premixer exit, where the flame is stabilized. The premixer is located coaxially near the inlet of a tube or the combustor shroud. The ambient air is entrained from the space between the premixer and combustor shroud. This air is denoted as the diffusion air or secondary air. The overall airflow rate and hence, the equivalence ratio is controlled by a variable speed suction fan located downstream of the combustor shroud. At a given fan speed, the split between the premixing air and diffusion air is determined by the distance (x) between the premixer and combustor shroud. The fuel nozzle and premixer were mounted rigidly on a traversing table with a stepper motor to vary this distance. In residential furnaces, the conditioning air is forced through the combustor shroud to extract thermal energy from the hot gases. In experiments, the ordinary tap water was circulated in a jacket around the combustor shroud to remove the thermal energy.

Propane gas supplied from a pressurized tank was used as the fuel. The fuel flow rate was regulated by a needle valve, and measured by a calibrated rotameter. The fuel ejected from a 2.4 mm ID circular nozzle at a velocity of 5.2 to 7.2 m/s, and a Reynolds number of 2800 to 3900. The power rating of the burner varied between 2.0 and 2.8 kW. The fuel and air were at typical ambient conditions of 25 C and 1 atm pressure. The distance between the fuel nozzle and premixer was 12 mm. The ID at the premixer inlet and exit was, respectively, 30 mm and 33 mm. The distance x varied from zero to 25 mm, and the maximum fan speed was 1600 rpm. The combustion process was fuel-lean at all operating points, with the overall equivalence ratio varying between 0.13 and 0.76. The split between the premixing air and diffusion air was not measured in this study. The flame was unstable at fan speeds close to 1600 rpm because the mixture exiting the premixer was highly fuel-lean. The flame blew-off at high fan speeds if the premixer was close to the combustor shroud (i.e. x = 0). The water flow rate was kept constant at 0.22 kg/s. The water temperature increased by 2 to 3 C depending upon the heat removed, which varied approximately from 60 to 80% of the energy released. Note that even though the combustion system used in this study is functionally different from gas turbine combustors, the concept to actively control the fuel-air premixing and overall equivalence ratio is applicable to lean-premixed combustors used in gas turbines.

Instrumentation

The combustor performance was monitored by a sampling probe and a thermocouple. The time-averaged measurements were taken at

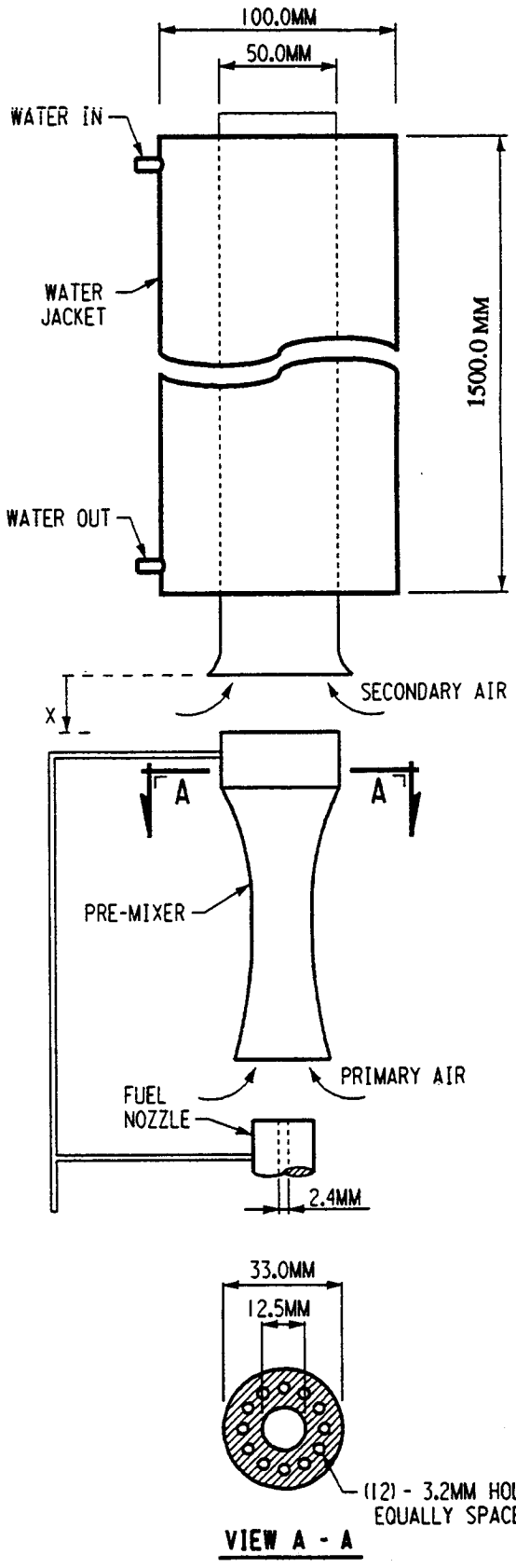

Figure 1. A Schematic of the Combustion System.

approximately 1.5 m downstream of the flame, allowing for one spatial data point to represent the average mixture value. The gas sample was drawn through a 6.4 mm diameter stainless steel probe with a 3.6 m long hose to cool the sample by ambient air before it reached a series of water traps and filters. The concentrations of O_2, CO and NOx (as NO) were measured by a Nova Analytical Systems Model 362. The full-scale of these electrochemical fuel-cell type sensors was, respectively, 25%, 2000 and 250 ppm. The sensors were accurate to +/- 0.1 percent, +/- 20 ppm and +/- 2 ppm. The CO emissions were monitored during experiments although they were inconsistent in the present setup. The product gas temperature was measured by a type-K thermocouple. Analog signals from the analyzer and thermocouple were digitized using a PC based data acquisition board by Strawberry Tree. Previous experiments (Padmanabhan et al. 1995; Davis and Samuelsen, 1996) have shown that repeatable measurements are necessary for controller to function properly. Therefore, we conducted several tests to determine the time required for such measurements. Based on these tests, the time-averaged value was obtained from data taken at 1 Hz for 1 minute. Measurements at a new operating point were initiated after a waiting period of 1 minute to reach steady state.

Control System

The control system performed three sequential tasks. First, it evaluated a cost function using outputs from performance sensors. Next, it executed a cost minimization algorithm to determine the premixer location and suction fan speed. Finally, the controller generated signals for actuators, which affected the primary and secondary airflow rates. A schematic of the control system is depicted in Fig. 2.

The cost function may take various forms depending upon the desired outcome. The objective of the present combustion system is to maximize heat transfer to the coolant, which normally coincides with a high combustion temperature. The high temperature however increases the NOx emissions, which must be limited. Accordingly, the combustor must operate fuel-lean (to ensure high combustion efficiency) and at the highest possible combustion temperature (i.e with the least amount of the excess air) while satisfying the NOx emission standard. Note that the oxygen concentration in products indicates the combustion temperature and overall equivalence ratio. Assuming complete

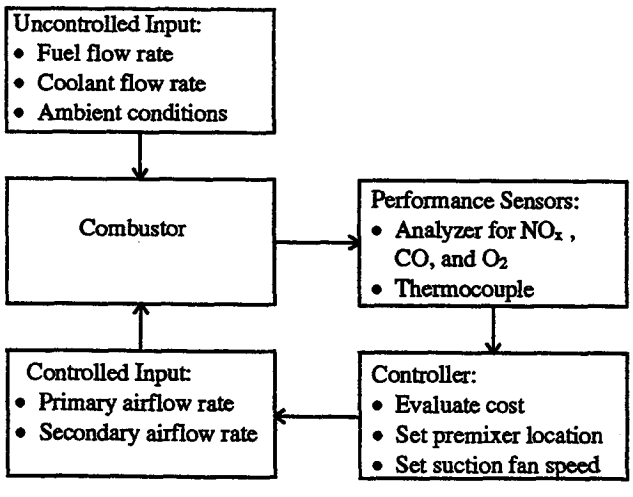

Figure 2. A Schematic of the Control Process.

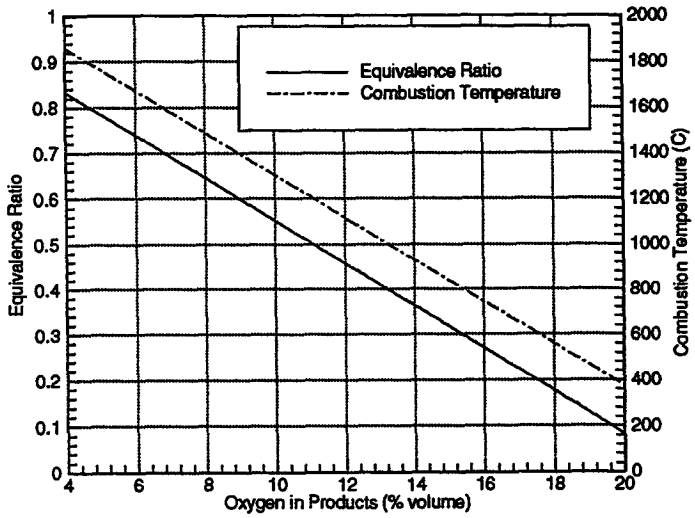

Figure 3. Equivalence Ratio and Combustion Temperature versus Oxygen in Products

combustion, the equivalence ratio (ER) is found from the equation

$$ER = 5(4.76X_{o_2} - 1)/(2X_{o_2} - 5) \quad (1)$$

where X_{o_2} is the oxygen mole fraction in products. Figure 3 plots the equivalence ratio and combustion temperature versus the percentage volume of oxygen ($100X_{o_2}$) in products. The combustion temperature is the adiabatic flame temperature assuming complete combustion.

The contradictory requirements discussed above were considered in the design of the cost function evaluated as

$$J = J_{O_2} + J_{NO_x} \quad (2)$$

where J_{O_2} is the percentage volume of oxygen in products normalized by its range of 5.5 to 18.5 percent. J_{NO_x} is the NOx penalty given as

$$\begin{aligned} J_{NO_x} &= 0.0 \quad && if\ NO_x \le 10ppm \\ &= 1.0 \quad && if\ NO_x > 10ppm \end{aligned} \quad (3)$$

Note that the combustor performance is affected by emissions of CO, UHC and soot etc., which were not accounted for explicitly in the cost function. The step function in Eq. 3 imposed a high cost if the NOx concentration exceeded 10 ppm. This is consistent with emission standards, which usually specify a limiting value. In Eq. 2, the cost function for oxygen varies linearly in the interval 0 to 1. Minimizing J in Eq. 2 optimizes the combustor performance. The present design of the cost function avoids the unstable combustion region (i.e. highly lean conditions), coinciding with the poor combustor performance (i.e. high volume of oxygen in products).

The cost function was minimized using the downhill simplex algorithm developed by Nelder and Mead (1965), and employed by Padmanabhan et al. (1995) for combustion control. Figure 4 shows a flow chart of the algorithm as implemented in this study. In a 2D system

with two control parameters, the algorithm begins by evaluating cost at three guess coordinate locations, which form a triangle or simplex. The algorithm searches through the domain to shrink the size of the simplex in successive iterations. At each iteration, the high cost vertex of the simplex is moved to a new location by reflecting, expanding, or contracting it with respect to the remaining vertices. The algorithm converges when the difference between the high and low costs of the simplex reduces to a specified tolerance.

The control parameters were the premixer distance (X) and suction fan speed (S) normalized by the maximum values of 25 mm and 1600 rpm, respectively. The physical constraints dictated that X and S vary between 0.0 and 1.0. The premixer will be damaged if it entered the combustor shroud, and the suction fan must not exceed the maximum rated speed. These constraints were imposed in the simplex algorithm by relocating at the boundary a vertex moving outside the boundary. However, this prompted the algorithm to get "stuck" when all 3 vertices were located at a boundary because the simplex reduced to a line. The problem was alleviated by adding a large penalty (1.0) to the cost function when the simplex attempted to move outside the physical boundaries. With this modification, the algorithm performed properly because the search beyond boundaries was costly and hence, it was rejected.

Each trial of the control algorithm produced new X and S values. The controller generated digital signals to drive the stepper motor to traverse the premixer to the new location X. An analog voltage signal was generated to change the fan speed to the desired value S. The control algorithm was coded in C (Press et al., 1992) and the control outputs were generated using PC based hardware from Strawberry Tree.

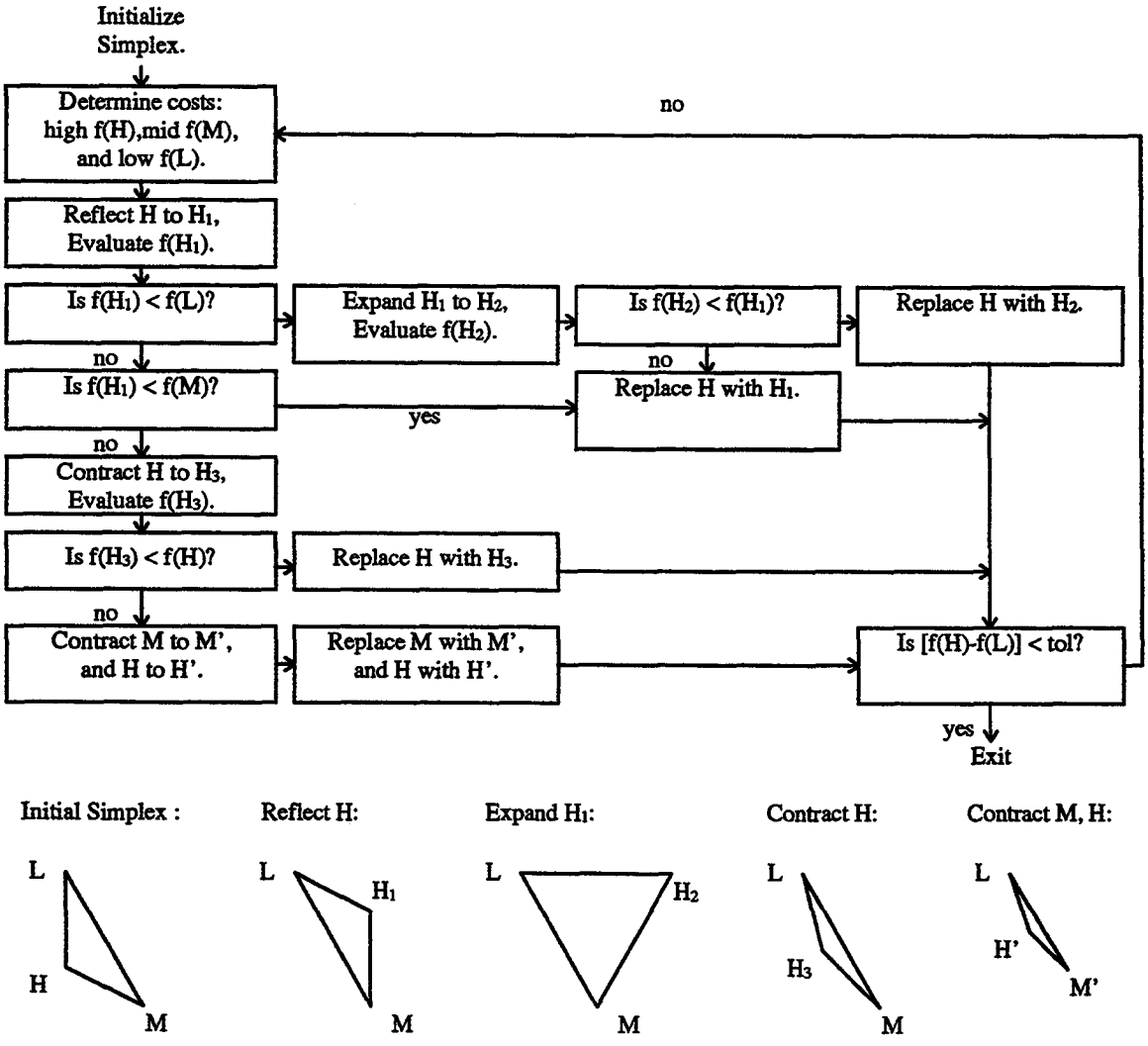

Figure 4. Flow Chart of the Downhill Simplex Algorithm.

RESULTS AND DISCUSSION

Experiments to demonstrate the controller were conducted at different fuel flow rates. A summary of the test conditions is shown in Table 1. For all test cases, the initial simplex was an equilateral triangle with vertex coordinates (X, S) located at (0.00, 0.00), (0.50, 0.00) and (0.00, 0.50). For each test case, we present the following results during the optimization: 1) the size and location of the simplex, 2) costs at the three vertices of the simplex, and 3) the sensor outputs at the high cost vertex of the simplex.

Figure 5(a) shows how the size and location of the simplex varied during optimization for Case 1. Each iteration narrowed the search space, which shifted towards a higher fan speed and smaller premixer distance. The algorithm converged after 12 iteration when the specified tolerance of 0.03 was satisfied at (0.06, 0.41), (0.05, 0.43) and (0.05, 0.43). Figure 5(b) shows the high, mid, and low costs at vertices of the simplex during iterations. The high and mid costs increased initially and decreased subsequently, as the simplex reached the optimal location with cost values of 0.67, 0.70, and 0.70. Cost higher than 1.0 indicates NOx greater than 10 ppm. Evidently, the low cost did not change noticeably because one of the initial vertices (0.00, 0.50) was near the optimal location. Figure 5(c) shows the NOx concentration, percentage volume of oxygen, and product temperature at the high cost point during iterations. Results at this point are most revealing because the control algorithm optimizes by relocating the high cost point. Initially, the NOx decreased from 26 ppm to 6 ppm as the volume percentage of oxygen increased from 6.7 to 15.4. Subsequently, the NOx increased gradually to the 10 ppm limit as the percentage volume of oxygen decreased marginally to 14.5 percent. The product temperature had a trend opposite to that of the percentage volume of oxygen. The optimal point with minimum cost corresponded to 10 ppm NOx, 14.2% volume of oxygen, and product temperature of 340 C. The optimal equivalence ratio and combustion temperature evaluated from Fig. 3 were 0.34 and 910 C, respectively. These results demonstrate that the controller maximized the combustion temperature while limiting NOx to within 10 ppm. The CO emissions ranged from 35 to 540 ppm, with a value of 40 ppm in the optimal regime.

Table 1. Summary of the Test Conditions

	Case 1	Case 2	Case 3
Fuel Flow Rate, kg/s*10^5	5.25	4.26	5.88
Fuel Jet Reynolds Number	3470	2815	3885
Air Flow Rate, kg/s*10^3	1.12 to 2.70	1.22 to 3.26	1.18 to 3.62
Equivalence Ratio	0.30 to 0.73	0.21 to 0.55	0.26 to 0.78
Power Input, kW	2.44	1.98	2.73

Fuel and Air Temperature	25 C
Operating Pressure	1 atm

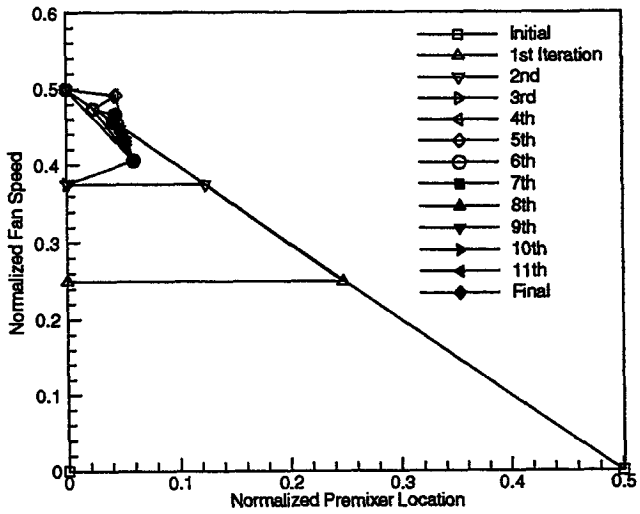

Figure 5(a) Simplex Location During Optimization (Case 1)

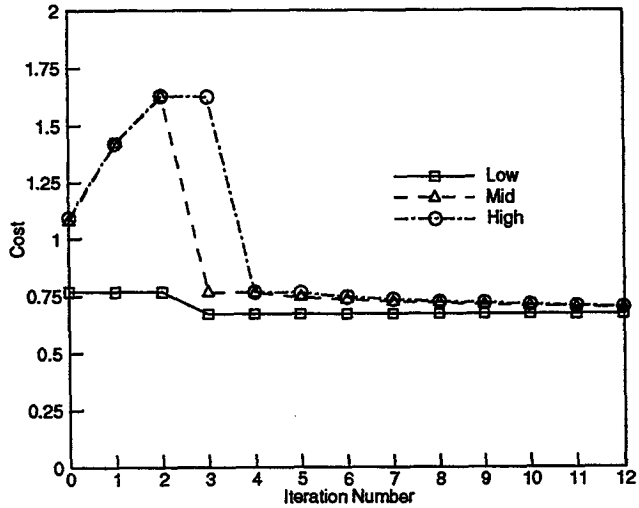

Figure 5(b) High, Mid and Low Costs of Simplex (Case 1)

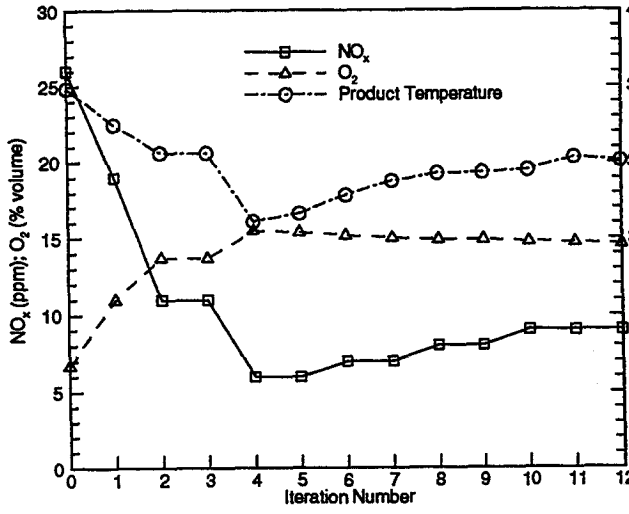

Figure 5(c) Sensor Output at the High Cost Point of Simplex (Case 1)

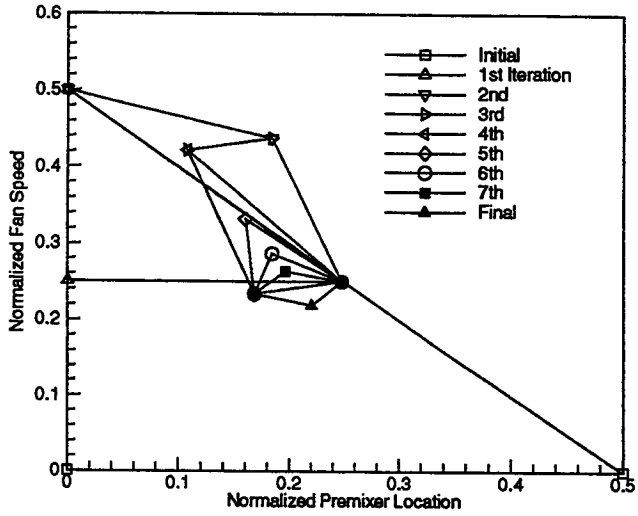

Figure 6(a) Simplex Location During Optimization (Case 2)

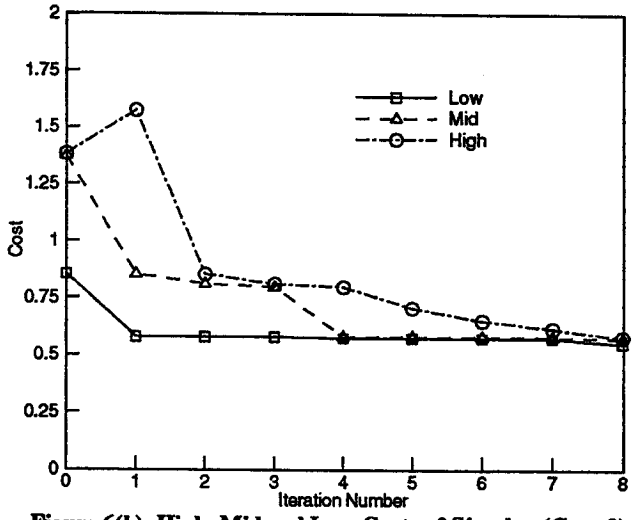

Figure 6(b) High, Mid and Low Costs of Simplex (Case 2)

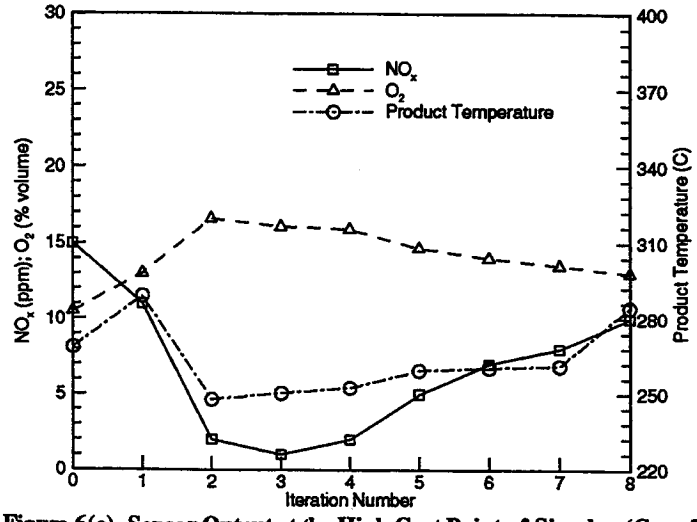

Figure 6(c) Sensor Output at the High Cost Point of Simplex (Case 2)

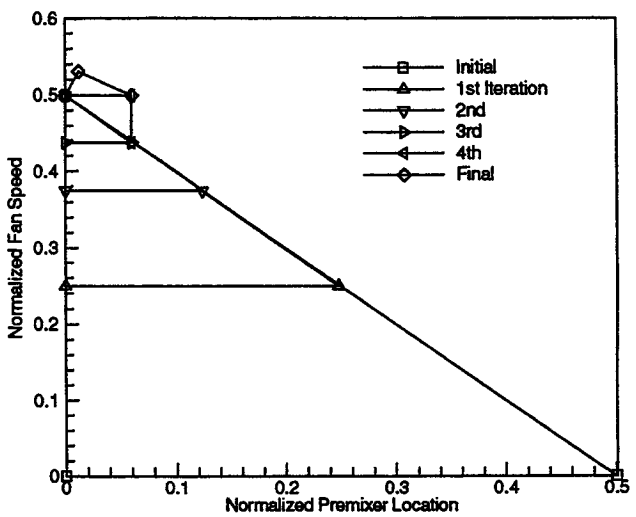

Figure 7(a) Simplex Location During Optimization (Case 3)

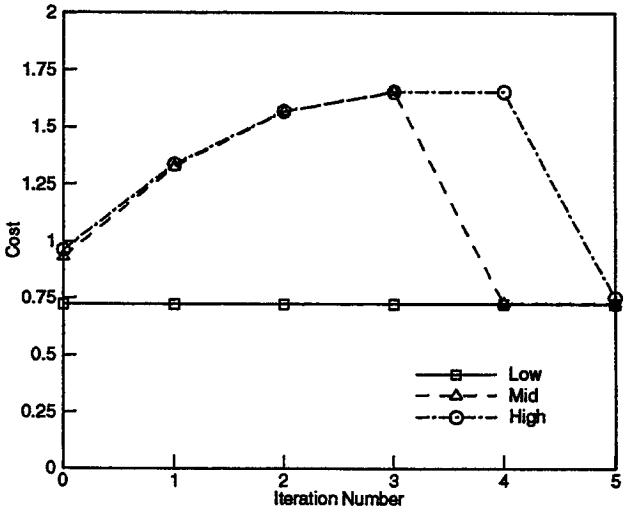

Figure 7(b) High, Mid and Low Costs of Simplex (Case 3)

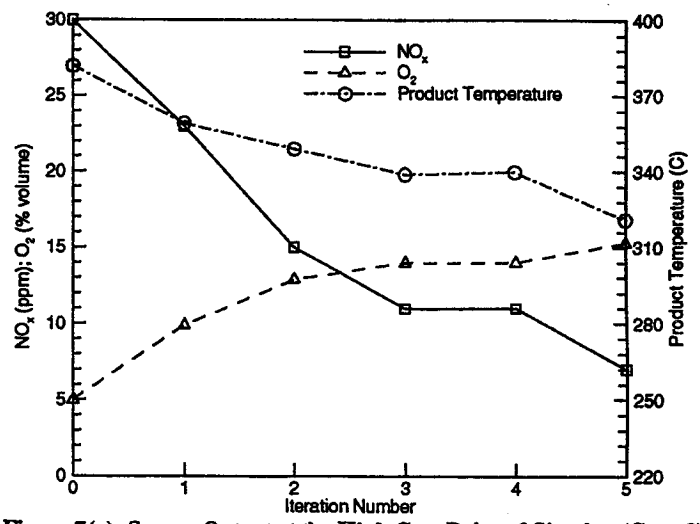

Figure 7(c) Sensor Output at the High Cost Point of Simplex (Case 3)

The test results at a lower fuel flow rate (Case 2) are shown in Figs. 6(a)-(c). The movement of the simplex during the optimization is tracked in Fig. 6(a), which reveals that the algorithm searched regions outside the initial simplex but it reverted back. The algorithm converged after 8 iterations when the simplex was located at (0.22, 0.22), (0.17, 0.23), and (0.25, 0.25). A lower fan speed and hence, a lower airflow rate, and larger premixer distance were required to achieve the optimal performance at a lower fuel flow rate. A larger size of the final simplex indicates that the cost function in the optimal region was less sensitive to the control parameters. Figure 6(b) shows the high, mid and low costs of the simplex during iterations. The cost decreased at all points to final low, mid and high values of, respectively, 0.55, 0.57, and 0.58. The NOx concentration in Fig. 6(c) decreased from a high of 15 ppm to a low of 1 ppm after 3 iterations. Subsequently, the algorithm responded by increasing NOx to the 10 ppm limit as the percentage volume of oxygen decreased. In agreement with Case 1, the product temperature had a trend opposite to that of the percentage volume of oxygen. The optimal point with the lowest cost resulted in 10 ppm NOx, 13.0% oxygen by volume, and product temperature of 260 C. The optimal equivalence ratio and combustion temperature were 0.40 and 1035 C, respectively. Note that the optimal combustion temperature was higher at the lower fuel flow rate. The CO emissions in the optimal regime varied from 50 to 80 ppm, with the overall range of 45 and 165 ppm.

As a final check, the fuel flow rate was increased in Case 3. Figure 7(a) shows that the optimization required 5 iterations to converge the simplex at (0.00, 0.50), (0.06, 0.50) and (0.01, 0.53), which is near one of the initial guess points. A higher airflow rate and smaller premixer distance were required to optimize the combustor performance at a higher fuel flow rate. According to Fig. 7(b), costs at the final simplex were 0.72, 0.72, and 0.75. As shown in Fig. 7(c), the NOx concentration at the high cost point decreased from 30 ppm to 7 ppm. The optimal point with the lowest cost corresponded to 10 ppm NOx, 14.9% volume of oxygen, product temperature of 328 C, equivalence ratio of 0.30, and combustion temperature of 820 C. The CO emissions in the optimal regime varied from 50 and 110 ppm, with the overall range of 50 and 850 ppm. A summary of results at the optimal point is shown in Table 2 for all test cases. Evidently, the optimal equivalence ratio and combustion temperature increased as the fuel flow rate was decreased.

Table 2. A Summary of Test Results at the Optimal Point

	Case 1	Case 2	Case 3
Normalized Premixer Location	0.05	0.21	0.06
Normalized Fan Speed	0.42	0.23	0.51
% Volume of Oxygen	14.2	13.0	14.9
Equivalence Ratio	0.34	0.40	0.30
Combustion Temperature, C	910	1035	820
Product Temperature, C	340	260	328

CONCLUSIONS

We have introduced active control to optimize combustor performance by articulating fuel-air premixing and combustion-zone stoichiometry. This flow articulation scheme is applicable to low-NOx lean-premixed combustors used in advanced gas turbines. The concept was used in a burner for residential furnaces. The control scheme located the design point for optimal performance at different fuel flow rates without prior knowledge of the system behavior. Following is a summary of the important observations.

- The cost function design is crucial to achieve the desired outcome. The cost function in this study represents a practical scenario; maximize the combustion temperature, and comply with the NOx emission standard. A limit of 10 ppm was arbitrarily chosen to demonstrate the controller. This limit will change to conform to a new regulation.

- The search algorithm avoided regions of poor combustion stability coinciding with a high volume of oxygen in products, which increased the cost. The controller rejected low fan speeds (or low airflow rates) producing high NOx and CO emissions.

- The controller searched regions outside the initial simplex. The search space was constrained by structural features of the combustor. The controller was prevented from moving outside the known physical boundaries. A cost function penalty was devised to prevent the controller from getting "stuck" at the boundary.

- The effect of the premixer location on the combustor performance was less significant except at low fan speeds. A smaller premixer distance decreased the total airflow rate, and increased the NOx production. Experiments providing independent measurements of the premixing airflow rate at different operating conditions are necessary to delineate the detailed mechanisms involved.

- The speed of the optimization was dictated by the time required to obtain repeatable measurements. This is not an issue in applications where the operating conditions change gradually and/or occasionally. Improving optimization speed using faster measurements requires optical techniques because sampling probes have inherently poor temporal response.

REFERENCES

Brouwer, J., Ault, B.A., Bobrow, J.E., and Samuelsen, G.S., 1990, "Active Control for Gas Turbine Combustors," Twenty-third Symposium (International) on Combustion, The Combustion Institute, Pittsburgh, pp. 1087-1092.

Davis, N.T., and Samuelsen, G.S., 1996, "Optimization of Gas Turbine Combustor Performance Throughout the Duty Cycle," Twenty-sixth Symposium (International) on Combustion, The Combustion Institute, Pittsburgh, pp. 2819-2825.

Kolluri, P., Kamal, A., and Gollahalli, S.R., 1996, "Application of Noncircular Primary-Air Inlet Geometries in the Inshot Burners of Residential Gas Furnaces," ASME Journal of Energy Resources Technology, vol. 118, pp. 58-64.

Maughan, J.R., Elward, K.M., DePietro, S.M., and Bautista, P.J., 1997, "Field Test Results of a Dry Low NOx Combustion System for the MS3002J Regenerative Gas Turbine," ASME Journal of Engineering for

Gas Turbines and Power, vol. 119, pp. 50-57.

McManus, K.R., Poinsot, T., and Candel, S.M., 1993, "A Review of Active Control of Combustion Instabilities," Progress in Energy and Combustion Science, vol. 19, pp. 1-29.

Nelder, J.A., and Mead, R., 1965, "A Simplex Method for Function Minimization," The Computer Journal, vol. 7, pp. 308-313.

Neumeier, Y., and Zinn, B.T., 1996, "Experimental Demonstration of Active Control of Combustion Instabilities using Real-Time Modes Observation and Secondary Fuel Injection," Twenty-sixth Symposium (International) on Combustion, The Combustion Institute, Pittsburgh, pp. 2811-2818.

Padmanabhan, K.T., Bowman, C.T., and Powell, J.D., 1995, "An Adaptive Optimal Combustion Control Strategy," Combustion and Flame, vol. 100, pp. 101-110.

Press, H.W., Saul, A.T., Vetterling, W.T., and Flannery, B.P., 1992, Numerical Recipes in C, The Art of Scientific Computing, Cambridge University Press, Cambridge.

Puri, R., Stansei, D.M., Smith, D.A., and Razdan, M.K., 1997, "Dry Ultralow NOx Green Thumb Combustor for Allison's 501-K Series Industrial Engines," ASME Journal of Engineering for Gas Turbines and Power, vol. 119, pp. 93-101.

Yamada, H., Shimodaira, K., and Hayashi, S., 1997, "On-Engine Evaluation of Emissions Characteristics of a Variable Geometry Lean-Premixed Combustor," ASME Journal of Engineering for Gas Turbines and Power, vol. 119, pp. 66-69.

Wilson, K.J., Gutmark, E., Schadow, K.C., and Smith, R.A., 1995, "Feedback Control of a Dump Combustor with Fuel Modulation," AIAA Journal of Propulsion and Power, vol 11, pp. 268-274.